Available online at www.sciencedirect.com

SCIENCE DIRECT®

Journal of Organometallic Chemistry 691 (2006) 3232–3238

Journal of Organo metallic Chemistry

www.elsevier.com/locate/jorganchem

Intramolecular carbonyl···carbonyl interactions in W, Mo and Fe complexes containing the η^1-*N*-maleimidato ligand: X-ray, DFT and AIM studies

Marcin Palusiak [a],*, Bogna Rudolf [b], Janusz Zakrzewski [b], Arno Pfitzner [c], Manfred Zabel [c], Sławomir J. Grabowski [a]

[a] *Department of Crystallography and Crystal Chemistry, University of Łódź, Pomorska 149/153, 90-236 Łódź, Poland*
[b] *Department of Organic Chemistry, University of Łódź, 90-136, Łódź, Poland*
[c] *Institute of Inorganic Chemistry, University of Regensburg, 93040 Regensburg, Germany*

Received 24 January 2006; received in revised form 10 March 2006; accepted 21 March 2006
Available online 3 April 2006

Abstract

The crystal structures of (η^5-C_5H_5)W(CO)$_3$(η^1-*N*-maleimidato) and (η^5-C_5H_5)Fe(CO)$_2$(η^1-*N*-maleimidato) complexes were determined by single crystal X-ray diffraction. The molecular geometries of both structures are compared with those of the Mo analog of the W complex and ethyl-*N*-maleimide in order to find a relation between the geometrical features and the rate constants of the addition reaction of the sulfhydryl group of biomolecules to the ethylenic bond of the maleimidato fragment. For a deeper insight into the problem DFT calculation were performed. An analysis of atomic charges, using the CHELPG scheme, and of theoretical electron density function, using the AIM theory, was performed. In the (η^5-C_5H_5)W(CO)$_3$(η^1-*N*-maleimidato), likewise in its Mo analog, the carbonyl···carbonyl interaction was found both for experimental and calculated structures. It is probably the first approach to explain this type of intramolecular interactions acting in organometallic compounds. This interaction can play the essential role in the reaction mechanism of nucleophilic addition to the maleimidato moiety. The AIM investigations indicate also the differences in the character of bonding between the η-*N*-maleimidato ligand and the central metal atom.

Keywords: Carbonyl···carbonyl interactions; Maleimidato ligand; DFT; AIM; X-ray structures

---

1. Introduction

Different types of weak bonding interactions are subject of numerous investigations in many branches of natural sciences. Among them are carbonyl···carbonyl interactions, which can be competitive with hydrogen bonds and similarly as the latter, can play an important role in many chemical, biochemical, or physical processes [1]. For example, it has been found that C=O···C=O interactions play the crucial role during the formation of cyanuric acid crystals [2–4]. Carbonyl···carbonyl interactions provide also important contributions to the shaping of secondary structures of proteins. It has been reported that $O_{carbonyl}\cdots C_{carbonyl}$ is a significant attractive interaction holding together α-helices and β-sheets [5–7]. It has been also found during studies of solvent effects, that solvents containing carbonyl groups form complexes with indanetrione derivatives via C=O···C=O contacts, influencing the electronic structures of the latter [8]. Usually, this kind of bonding is considered as mainly electrostatic, especially for long distances between interacting atoms, when the coulombic forces dominate. The intramolecular carbonyl···carbonyl interactions in organometallic derivatives of maleimide are investigated here. To the best of our knowledge this is the first report dealing with this type of interactions acting in organometallic compounds.

Maleimido compounds are often used for the selective alkylation of thiol-containing biomolecules [9]. Covalently

---

* Corresponding author. Tel.: +48426355740; fax: +48426790447.
E-mail address: marcinp@uni.lodz.pl (M. Palusiak).

0022-328X/$ - see front matter © 2006 Elsevier B.V. All rights reserved.
doi:10.1016/j.jorganchem.2006.03.035

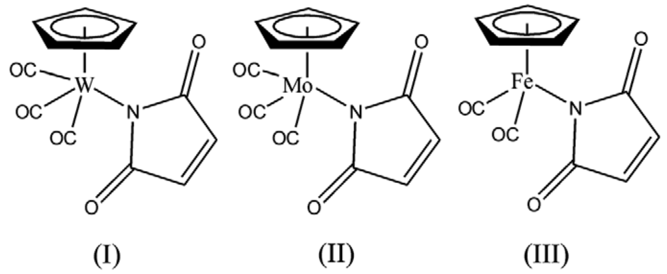

(I) (II) (III)

Chart 1.

labelled biomolecules with transition metal complexes are very interesting species because their unusual redox properties [10], IR absorption [11] or luminescence features [12–14] enable their sensitive detection in biological samples. The reaction rates of transition metal complexes containing the maleimidato ligand with thiol groups in biomolecules were already investigated. It has been reported for the molecular structure of the (η^5-C_5H_5)Mo$(CO)_3$(η^1-*N*-maleimidato), that two of three carbonyl groups coordinating molybdenum are interacting with $O_{carbonyl}$ atoms of the maleimidato ligand [15]. It was suggested that since this interaction is intramolecular, it can have impact on the reactivity of this compound in a nucleophilic addition reaction of the maleimidato fragment to the ethylenic bond. Here, the molecular structure of (η^5-C_5H_5)W$(CO)_3$(η^1-*N*-maleimidato) (**1**), the tungsten homologue of the (η^5-C_5H_5)Mo$(CO)_3$(η^1-*N*-maleimidato) (**2**), as well as the related complex with iron as the central atom, (η^5-C_5H_5)Fe$(CO)_2$(η^1-*N*-maleimidato) (**3**), is reported (see Chart 1 with schemes of **1**–**3**). The geometrical features of the above-mentioned Mo derivative and *N*-ethylmaleimide as the maleimidato moiety in typical organic compound [16] were also taken into consideration. The rate constants and half-live times are explained by the geometrical data estimated on the basis of X-ray investigations. The studies are widened by quantum chemical calculations for Mo, W and Fe organometallic systems as well as for *N*-ethylmaleimide. The computations are carried out on the basis of density functional theory [17,18] and the quantum theory "Atoms in Molecules" [19,20].

2. Experimental

2.1. X-ray investigations

For details of the syntheses of the organometallic derivatives see Ref. [15]. Crystals of **1** and **3** were obtained by slow evaporation of aqueous solutions. Single crystals suitable for X-ray measurement were mounted on glass-fibres. X-ray diffraction data were collected at 170 K on a STOE IPDS I using Mo Kα radiation. The unit cells were determined from 8000 reflections. Both crystal structures were solved by direct methods and then refined by full-matrix least-squares methods against F^2. All hydrogen atoms were placed on geometrically idealized positions and constrained to ride on their parent atoms, with a C—H distance of 0.950 Å and $U_{iso}(H) = 1.2U_{eq}(C)$. Selected crystal data are collected in Table 1. Table 2 contains selected geometrical parameters.

Table 1
Crystallographic data and structure refinement

Compound	1	3
Formula	$C_{12}H_7N_1O_5W_1$	$C_{11}H_7N_1O_4Fe_1$
Molecular weight (g cm^{-3})	429.04	273.03
Crystal system	Monoclinic	Triclinic
Space group	$P2_1/c$	$P\bar{1}$
a (Å)	14.386(2)	6.3896(11)
b (Å)	8.6877(6)	7.4671(16)
c (Å)	15.747(3)	11.885(2)
α (°)	90.0	83.00(2)
β (°)	142.385(6)	88.10(2)
γ (°)	90.0	70.74(2)
V (Å^3)	1201.2(3)	531.33(18)
Z	4	2
D_x (g cm^{-3})	2.372	1.707
μ (mm^{-1})	9.632	1.419
T (K)	173(2)	173(2)
λ (Å)	0.71073	0.71073
Index ranges	$-17 \leqslant h \leqslant 17$, $-9 \leqslant k \leqslant 10$, $-19 \leqslant l \leqslant 19$	$-7 \leqslant h \leqslant 7$, $-9 \leqslant k \leqslant 9$, $-14 \leqslant l \leqslant 14$
Number of unique data collected	2255	1920
Number of $I > 2\sigma(I)$ data	1868	1172
Number of parameters	172	154
R_1 [$I > 2\sigma(I)$]	0.0266	0.0425
wR_2 [$I > 2\sigma(I)$]	0.0611	0.0838
$\Delta\rho_{min}$ (e Å^{-3})	−0.616	−0.316
$\Delta\rho_{max}$ (e Å^{-3})	1.842	0.469

Table 2
Bond lengths (Å) in the maleimidato moiety and reaction rate constants for the investigated metal complexes and *N*-ethylmaleimide

d	1	2	3	*N*-ethylmaleimide[a]
N10—C11	1.398(7)	1.389(3)	1.407(6)	1.396
N10—C14	1.389(8)	1.394(3)	1.386(6)	1.378
C11—O11	1.207(8)	1.216(3)	1.220(6)	1.201
C14—O14	1.209(7)	1.213(3)	1.218(6)	1.198
C11—C12	1.517(9)	1.488(4)	1.510(6)	1.491
C13—C14	1.502(8)	1.482(4)	1.520(7)	1.487
C12—C13	1.321(10)	1.315(4)	1.316(8)	1.314
$t_{1/2}$ (min)	5.8	9.0	26.0	1.00
k	1732	1111	382	9532

[a] Esd's for *N*-ethylmaleimide are unavailable.

Rate constants and half-lives of reaction of the *N*-ethylmaleimide metal complexes under discussion with glutathione were determined in a water–methanol mixture (9:1) at pH 7.4 and 24 °C. For more experimental details see Ref. [15].

2.2. Computations

Geometries both for metal complexes and for *N*-ethylmaleimide were fully optimized using DFT methods in the GAUSSIAN-03 set of codes [21]. The starting geometries were taken directly from the crystal structures. The B3LYP functional [22–24] was applied with the 6-311+G(d) basis set [25,26] for C, N, O and H atoms and the LanL2DZ basis set [27–29] for the transition metals.

ECP corrections were applied for the latter using LanL2DZ pseudopotentials for core electrons. Wave functions and atomic charges were obtained at the same level of approximation. Population analysis was made using the CHELPG [30] scheme implemented in GAUSSIAN-03. The AIM2000 package [31] was applied for topological analysis of the theoretical electron density function.

3. Results and discussion

3.1. Crystal structures of the W and Fe complexes

In **1** the tungsten atom is coordinated by *Cg* of the cyclopentadienyl ring at the apex and three carbonyl groups and a nitrogen atom of maleimidato ligand in the basal positions of a square pyramid (a "four-legged piano stool structure"). Such an arrangement of ligands is in agreement with general observations for this type of coordinating environment. The basal bonds are tilted from the plane of the pyramid base. Distances between the carbonyl ligand carbon atoms and the central atom in the range of 2.009–2.032 Å are close to the average value of this parameter observed in related structures. For example, the average C(carbonyl)—W distance for 1798 (7239 matches) high quality crystal structures ($R < 5\%$, without unresolved errors, no reported structural disorder, without polymeric or powder structures) found in CSD [32] amounts to 2.007(41). The distances $C{=}O\cdots C_{(carbonyl)}$ of 2.796(13) Å and 2.921(15) Å for O(14)···C(20) and O(11)···C(40) suggest the possibility of the existence of intramolecular carbonyl···carbonyl interaction, which can be competitive with hydrogen bonds as already proved both by using the CSD crystallographic data and ab initio calculations [1]. The carbonyl ligand C30—O30 forms an almost straight line with the central metal atom, i.e. the angle O30—C30···W is 177.3(6)°, while both other CO groups are clearly out from this linear orientation. The corresponding angles are 172.8(5)° and 173.0(5)° for O20—C20···W and O40—C40···W, respectively. Moreover, the carbon atoms C20 and C40 are clearly oriented towards the oxygen atoms of the maleimide ligand, which also can suggest the existence of mentioned carbonyl···carbonyl interaction. Since these effects are intramolecular, they may occur not only in the solid state, but also in solution, and may influence the reactivity of the maleimide moiety. As it was mentioned above, such a type of carbonyl···carbonyl interaction was already reported for the homologue of **1** with Mo as central atom [15]. Generally, **1** and **2** homologues have very similar geometrical features, including potential intramolecular interactions. The situation is slightly different in the case of **3**. The iron atom is coordinated by *Cg* of the cyclopentadienyl ring at the apex and two carbonyls and a nitrogen atom of the maleimidato ligand in the basal positions of the trigonal pyramid (a "three-legged piano stool structure" in this case). Likewise in **1**, the basal bonds are tilted from the plane of the pyramid base distorting the pyramidal arrangement of the three basal ligands with respect to the central atom. The $C_{carbonyl}$—Fe bond lengths are in very good agreement with data collected in CSD. The mean value of Fe—C bond lengths in CSD data (2725 high quality crystal structures and 10 000 matches) is 1.784(28) Å while the corresponding values in the reported structure are 1.784(6) Å and 1.789(5) Å for C(10)-Fe and C(20)—Fe, respectively.

Table 2 contains values of quantities describing the reactivity of the complexes under discussion with glutathione and geometrical parameters of the maleimidato ligand in the corresponding metal complexes. These values are also compared with the corresponding data for *N*-ethylmaleimide. One can see that only in the case of the C11—O11 and C14—O14 carbonyl groups there is some correlation between bond lengths and reaction rates. All other geometrical parameters seem to change beyond any dependence. Generally, the geometrical differences of the maleimidato moiety in the considered molecules are not significant, especially if one takes into account the estimated standard deviations. However, it is worth mentioning that only in the case of the carbonyl C—O bond lengths in the maleimide moiety there is any observable relation with reaction rate constants.

Observations made for crystal structures give no distinct indication of the role of a potential carbonyl···carbonyl interaction inside the investigated samples, so the crystallographic measurements have been used as a starting point for deeper analysis with the usage of computational methods.

3.2. Atomic charge analysis

Atomic charges were estimated for **1**, **2**, and **3** as well as for *N*-ethylmaleimide, using the CHELPG scheme (CHarges from ELectrostatic Potentials using a Grid based method [30]) implemented in GAUSSIAN-03. These charges were evaluated at the same level of approximation as the optimizations of geometries were made. This method of population analysis was chosen since the corresponding results depend only slightly on the level of the applied approximation (method and basis set) as well as the charges calculated in such a way are of the relatively high reliability of obtained results [33,34]. The radii for W, Mo, and Fe were substituted by the values of distances between the atoms in crystals of tungsten (2.741 Å), molybdenum (2.725 Å) and iron (2.482 Å) according to *Table of interatomic distances and configuration in molecules and ions* [35] since other van der Waals radii for transition metals are not available. The calculated atomic charges are collected in Table 3. The atom numbering scheme is the same as that one in the experimental crystal structures (see Fig. 1).

As one can see in Table 3, there is a positive charge concentration on the carbonyl C atoms. Simultaneously, the negative charges are located mainly on the N and O atoms. Moderately negative atomic charges characterize those carbon atoms which are the centers of reactivity in the reac-

Table 3
CHELPG atomic charge values

		1	2	3	N-ethylmaleimide
	Metal atom	0.126	0.111	−0.051	–
Cyclopentadienyl ring	C1	0.020	0.034	−0.130	–
	C2	−0.139	−0.148	0.000	–
	C3	−0.053	−0.049	−0.108	–
	C4	−0.059	−0.050	−0.102	–
	C5	−0.135	−0.154	−0.009	–
Maleimidato ligand	N10	−0.553	−0.561	−0.393	−0.438
	C11	0.672	0.664	0.617	0.661
	O11	−0.525	−0.529	−0.547	−0.518
	C12	−0.206	−0.195	−0.228	−0.223
	C13	−0.237	−0.245	−0.218	−0.217
	C14	0.712	0.713	0.613	0.653
	O14	−0.543	−0.546	−0.546	−0.518
Carbonyls	C20	0.234	0.240	0.328	–
	O20	−0.215	−0.201	−0.215	–
	C30	0.270	0.269	0.326	–
	O30	−0.259	−0.242	−0.212	–
	C40	0.232	0.239	–	–
	O40	−0.215	−0.201	–	–

tion with the thiol group. Interestingly, there are only small differences between the atomic charge values for these carbon atoms in the investigated metal complexes and *N*-ethylmaleimide in comparison with the differences between the reaction rate constants. This finding as well as the charge distribution in the maleimidato ligand may suggest that whole of the $O{=}C{-}C{=}C{-}C{=}O$ sequence of atoms in the maleimidato moiety plays a significant role in the reaction mechanism. This observation can also be supported by the fact that only in the case of the carbonyl $C{-}O$ bond lengths in the maleimide moiety there is any observable relation with reaction rate constants, as it was mentioned in the previous section. The analysis of charge distribution in this part of investigated molecules allows to suspect that the process of nucleophilic addition to maleimidato moiety is analogous to the mechanism of reaction of conjugated nucleophilic addition to α,β-unsaturated aldehydes and ketones. The probable mechanism of such reaction has been shown on Fig. 2. The positive charge located on the $C_{carbonyl}$ atoms of maleimidato moiety favors the formation of the transition state.

It is well known, that CO ligands are σ-donating, but π-accepting moieties. On the other hand, it has been reported in the literature that the imidato ligand shows σ and π-donor properties [36]. Hence one could expect that *trans* carbonyl carbon atom in **1** and **2** will be less positive than its *cis* counterparts due to the transfer of electrons from imidato ligand to *trans* CO ligand. Meanwhile in both, **1** and **2** the *trans* $C_{carbonyl}$ atom is endowed with the greater positive charge surplus than equivalent C atoms in *cis* positions. Therefore, one may suspect that this is the effect of a partial charge transfer from the oxygen to the carbon atom in a carbonyl···carbonyl interaction. In the light of such observations the intramolecular $O_{carbonyl}\cdots C_{carbonyl}$ contact found in the molybdenum and tungsten derivative may significantly participate in the delocalization of the surplus charge in the transition form that is built during the reaction of the title compounds with L-cysteine or glutathione.

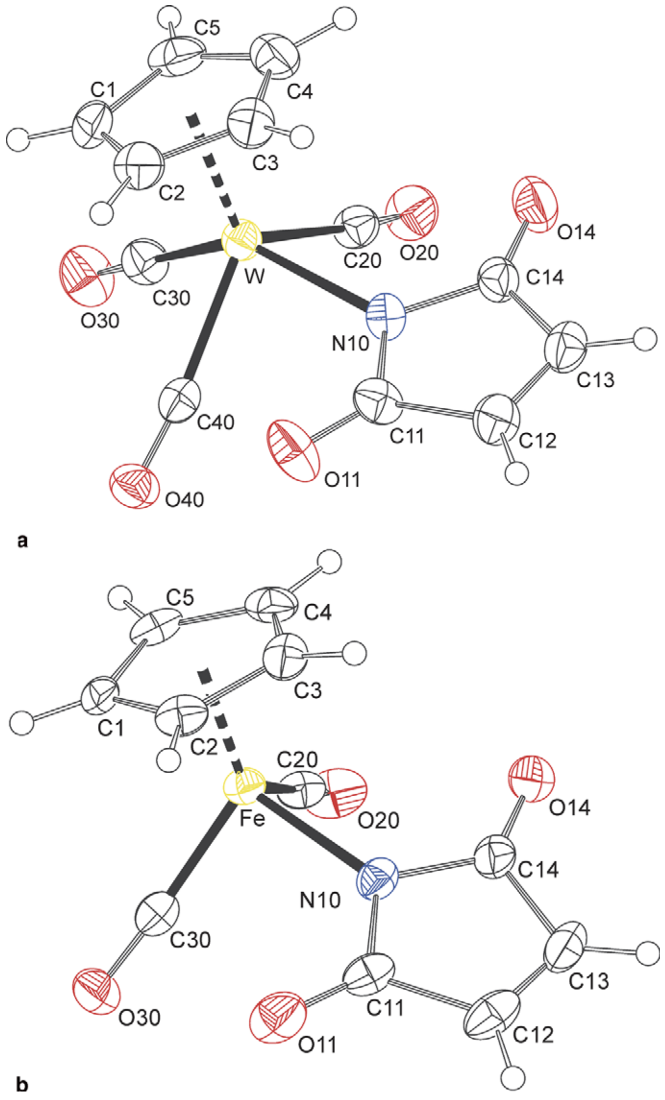

Fig. 1. View of **1** (a), and **3** (b), with atom labeling scheme. Ellipsoids are drawn at 40% probability.

3.3. AIM analysis

A detailed topological analysis of the electron density was performed on the basis of the "Atoms in Molecules" quantum theory. The wave functions were obtained at the same level of approximation as the optimization procedure was performed. The values of the electron density, the laplacian of the electron density and the ellipticity of bonds were analyzed.

There are four characteristic types of critical points in the AIM topological analysis of the electron density; the attractors, which are the local maxima of electron density

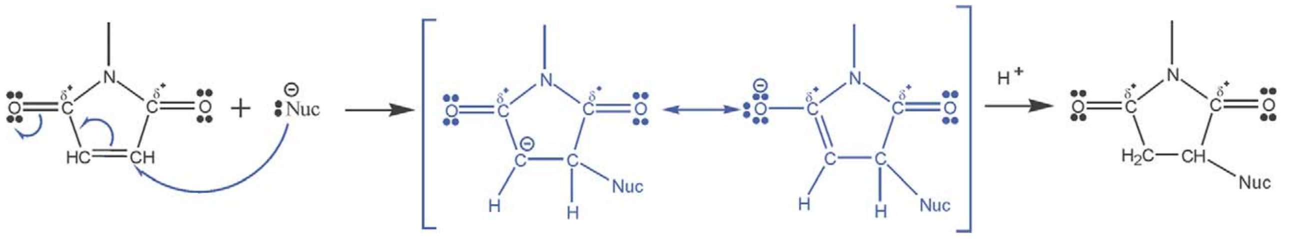

Fig. 2. Reaction scheme of the nucleophilic addition to the maleimidato moiety.

usually corresponding to the positions of atoms, then two types of saddle points, which correspond to local extremes of the electron density function characteristic for chemical bonds (bond critical points, BCP) and ring systems (ring critical points, RCP), and finally the cage critical points (CCP) [19,20]. In the case of the investigated systems there is a certain discrepancy with the general rule according to which all atoms are represented by atomic attractors. The metal atoms are represented by cage critical points surrounded by several non-atomic attractors and critical points (see Fig. 3). This is an artefact arising from approximations based on pseudopotential corrections for heavy atoms. The metal valence shell has its own topology, since there are regions of concentrations and depletions of valence electrons in the field of potential. The calculations made for **3** with usage of different basis sets for iron indicate that for the 6-311+G* basis set there is one attractor corresponding to the Fe atom. For the same basis set with the pseudopotential approximation (LanL2DZ) the metal valence shell has its own topology and the same is observed if the LanL2DZ basis set with pseudopotential approximation (also LanL2DZ) is applied. However, it should be pointed out that in the case of molybdenum and even more in the case of tungsten the correction for relativistic effects is an important approximation at all. Moreover, the 6-311G basis is unavailable for these atoms. On the other hand, the above-quoted calculations for **3** indicate that the differences in the quantities characterizing the critical points are very small for compared levels of calculations and mainly concern the closest surroundings of the iron

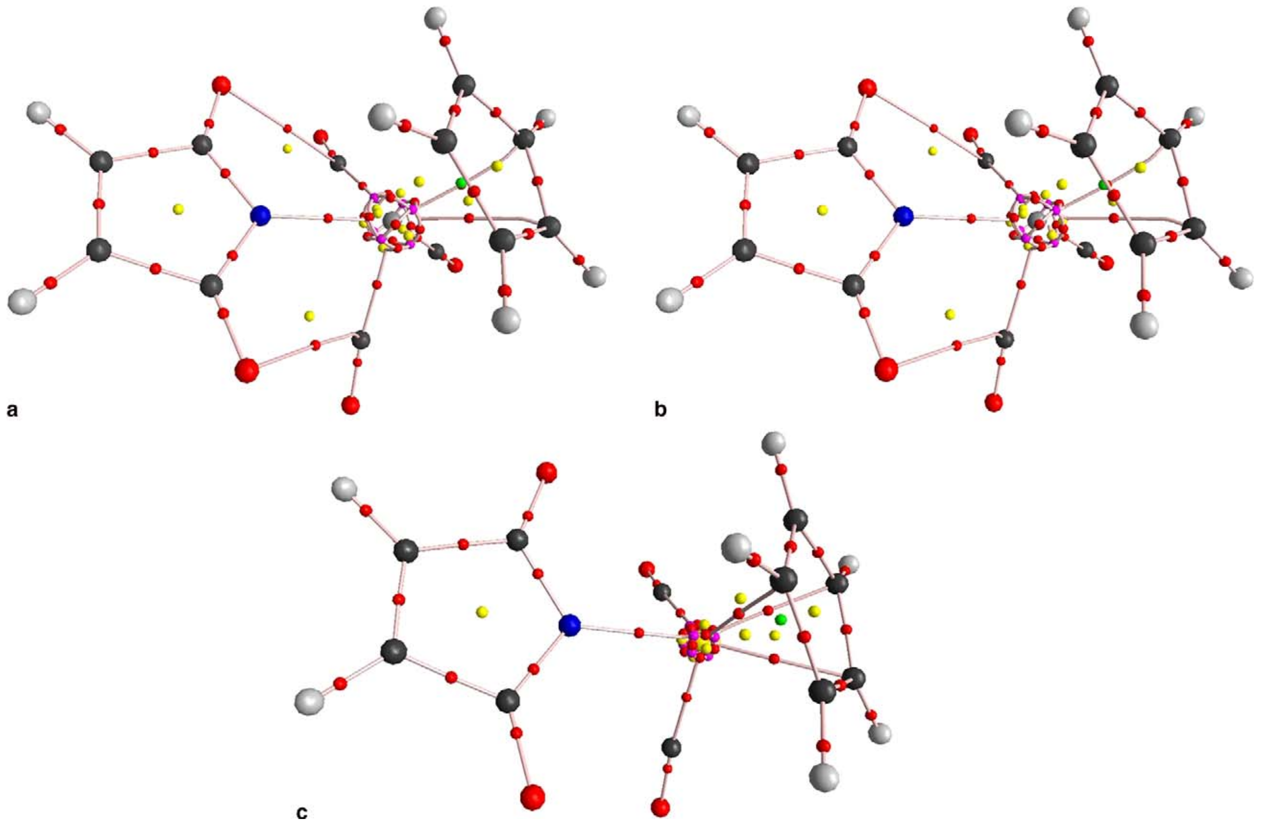

Fig. 3. Molecular graph of the **1** (a), **2** (b) and **3** (c); big circles correspond to atom positions, small ones are the critical points (BCPs red, RCPs yellow and CCPs green). In the case of (a) and (b) there are BCPs present with bond paths corresponding to carbonyl···carbonyl interactions. The electron density descriptors for these critical points are as follows: (a) $\rho_{O\cdots C} = 0.0149$ a.u., $\nabla^2\rho_{O\cdots C} = 0.0494$, $\varepsilon_{O\cdots C} = 0.4802$ and $\rho_{O\cdots C} = 0.0134$ a.u., $\nabla^2\rho_{O\cdots C} = 0.0451$, $\varepsilon_{O\cdots C} = 0.5877$; (b) $\rho_{O\cdots C} = 0.0154$ a.u., $\nabla^2\rho_{O\cdots C} = 0.0502$, $\varepsilon_{O\cdots C} = 0.4015$ and $\rho_{O\cdots C} = 0.0135$ a.u., $\nabla^2\rho_{O\cdots C} = 0.0445$, $\varepsilon_{O\cdots C} = 0.4831$. (For interpretation of the references to colour in this figure legend, the reader is referred to the web version of this article.)

atom (a maximum difference of circa 3% has been found for the electron density and its laplacian at $BCP_{(N–Fe)}$).

AIM theory has been found a very useful utility in the investigations of many weak intra- and intermolecular interactions, particularly hydrogen bonds [37]. Generally, it is possible to state on the basis of AIM theory that if there is a critical point with a corresponding bond path between two chemical individuals there should be some chemical bond between them. Furthermore, parameters of the electron density function in BCP may characterize properties of a bond or can be used for estimating its energetic properties. It was found for example that the electron density and its laplacian in BCP of a hydrogen bond correlate very well with energetic parameters of this interaction [38]. Thus, it is worth to realize such analysis for carbonyl⋯carbonyl contact found in the investigated molecules. Fig. 3(a) and (b) shows that in the case of tungsten and molybdenum derivatives the BCPs with corresponding bond paths connecting O atoms in the maleimide ligand and $C_{carbonyl}$ atoms are present. The electron density value at these BCPs equals approximately $\rho = 0.014$ a.u. (see the caption of Fig. 3). For comparison, the electron density at the BCP of a hydrogen bond in the water dimer (B3LYP/6-311+g(d) level of calculations, binding energy corrected by basis set superposition error $E_{bin} = 5.966$ kcal/mol) equals 0.026 a.u. This comparison may provide a rough estimation of energetic parameters of the discussed interaction. One should note, however, that the character of both types of interactions may differ significantly. For example, the binding energy in LiF, mainly erasing from coulombic forces, is close to 135.78 kcal/mol while ρ in $BCP_{Li–F}$ amounts to 0.06943 a.u. (B3LYP/6-311+g(d) level of calculations). In case of the discussed interaction, as it was repeatedly reported, especially for C═O⋯C═O interactions in proteins, the electrostatic forces may have the significant impact, which can be partially confirmed by the atomic charge distribution analyzed in the previous section. Also the laplacian values of ρ at $BCP_{carbonyl\cdots carbonyl}$ are positive. This is characteristic for closed-shell interactions, such as ionic interactions, hydrogen bonds or van der Waals interactions. Interestingly, the values of the ellipticity ε at the carbonyl–carbonyl BCP significantly differ from zero (this parameter illustrates how the electron density shape is flattened crosswise the bond path in BCP; ε equals zero for ideally cylindrical bonds, e.g. single CC or triple CC bonds, and differs from zero when the bond cross-section is elliptic). This indicates that the electron density shape is considerably flattened crosswise the bond path. It can be connected with some type of coupling with the metal valence shell localized closely to the interacting O and C atoms. The effect seems to be stronger in the case of the tungsten derivative. It should be pointed out that in the Fe complex the bond paths and hence the corresponding BCPs for carbonyl⋯carbonyl contacts are not observed.

It was mentioned in the previous section, the imidato ligand shows σ-donor and π-donor properties [36]. This can be confirmed by the analysis of the ellipticity at BCP of the N–metal bond. Interestingly, the Fe─N bond is almost ideally cylindrical. The ellipticity in $BCP_{Fe–N}$ is equal to $\varepsilon_{Fe–N} = 0.0179$ ($\rho_{Fe–N} = 0.0965$ a.u., $\nabla^2\rho_{Fe–N} = 0.3836$). The corresponding values for the Mo─N and W─N bonds are as follows: $\varepsilon_{Mo–N} = 0.3383$ ($\rho_{Mo–N} = 0.0785$ a.u., $\nabla^2\rho_{Mo–N} = 0.2795$) and $\varepsilon_{W–N} = 0.3402$ ($\rho_{W–N} = 0.0838$ a.u., $\nabla^2\rho_{W–N} = 0.2747$). This means that the relatively greatest contribution of π electrons in a metal–N bond is observed for (η^5-C_5H_5)W$(CO)_3$(η^1-*N*-maleimidato). In the case of (η^5-C_5H_5)Mo$(CO)_3$(η^1-*N*-maleimidato) the contribution is smaller but still comparable to that in the W complex. The Fe─N bond seems to be formed only by the σ orbital of nitrogen with a very small contribution of π electrons. It can be connected with the fact that, as distinct from **1** and **2**, in **3** there is no π-accepting CO ligand in the *trans* position.

Another interesting feature was observed for the analyzed metal complexes. One can see (Fig. 3) that there are only two bond paths in **1** and **2**, and three bond paths in **3**, connecting the central metal atom and the C atoms in the cyclopentadienyl rings. This could suggest that the central atoms are η^2-C_5H_5 or η^3-C_5H_5 coordinated. However, it should be also pointed out that the Pointcaré-Hopf relationship determining the mutual ratio of possible critical points in a non-periodic system is not fulfilled in case of the investigated organometallic systems. This means that the set of found critical points is incomplete. Yet, even individual iterations with highly defined grid-search and with the starting points in the midpoints between the positions of attractors corresponding to suitable C atoms in cyclopentadienyl rings and the position of the metal nucleus have not provided any new critical points. The situation is additionally complicated because of the untypical representation of metal atoms. There is a difficulty in the interpretation of the local topology of metal valence-shell regions deriving from EPS approximations. Nevertheless, if one analyzes the distribution of atomic charges located on the C atoms in the cyclopentadienyl rings, then one can find some relation in those values and the occurrence of the corresponding metal–C bond paths. It is worth mentioning here, that both in crystal structures and in theoretically investigated systems there is observed an asymmetry in metal–π bonding. In **1** and **2** the distance C3–metal is about 0.1 Å longer than the corresponding distances C1–metal and C5–metal. In the case of **3** these differences in metal–π bond lengths of about 0.05 Å are not so significant, but also observable. Generally, it is possible to state that the particular contributions of *Cp* carbon atoms in π–metal coordination are not equivalent.

4. Conclusions

It was found that in both **1** and **2** in the solid state there are intramolecular carbonyl⋯carbonyl interactions, for which the distances between the oxygen atoms in the maleimide ligand and the carbon atoms of carbonyl ligands are shorter than the corresponding sum of van der Waals radii. Also the other geometrical parameters indicate the existence of such interactions. There are similar findings for DFT fully optimized geometries of these metal complexes. The Atoms in Molecules analysis proofs, that there are *bond critical points* and the corresponding *bond paths* present for these interactions. The laplacians at these critical points are positive, which is typical for closed-shell interactions. The hypothetical mechanism of nucleophilic addition to maleimidato ligand has been derived. It seems that the carbonyl···carbonyl interactions can additionally stabilize the active transition form in this reaction. In the case of **3**, which shows the lowest reactivity in the considered reaction, these carbonyl···carbonyl interactions are not present.

Acknowledgements

M.P. and S.J.G. thank the Rector of the University of Lodz for financial support (University Research Grants – Grant No. 505/675 2005). Calculations have been carried out in the Warsaw (ICM) Supercomputer Center (Project: G29-5).

Appendix A. Supplementary data

Detailed crystallographic data can be obtained from The Cambridge Crystallographic Data Centre. CCDC Deposition numbers CCDC 290116 and CCDC 290117 for **1** and **3**, respectively. Supplementary data associated with this article can be found, in the online version, at doi:10.1016/j.jorganchem.2006.03.035.

References

[1] F.H. Allen, C.A. Baalham, J.P.M. Lommerse, P.R. Raithby, Acta Crystallogr., Sect. B 54 (1998) 320.
[2] H. Dietrich, C. Scheringer, H. Meyer, K.-W. Schulte, A. Schweig, Acta Crystallogr., Sect. B 35 (1979) 1191.
[3] A. Kutoglu, E. Hellner, Acta Crystallogr., Sect. B 34 (1978) 1617.
[4] G.C. Verschoor, E. Keulen, Acta Crystallogr., Sect. B 27 (1971) 134.
[5] P.I. Lario, A. Vrielink, J. Am. Chem. Soc. 125 (2003) 12787.
[6] P.H. Maccallum, R. Poet, J. Milner-White, J. Mol. Biol. 248 (1995) 361.
[7] P.H. Maccallum, R. Poet, J. Milner-White, J. Mol. Biol. 248 (1995) 374.
[8] J. Roy, S. Bhattacharya, S. Ghosh, D. Majumder, S.P. Bhattacharyya, Chem. Phis. 222 (1997) 161.
[9] G.T. Hermanson, Bioconjugate Techniques, Academic Press, San Diego, CA, 1996.
[10] D.R. Van Staveren, N. Metzler-Nolte, Chem. Rev. 104 (2004) 5931.
[11] M. Salmain, G. Jaouen, C.R. Chimie 6 (2003) 249.
[12] X.Q. Guo, F.N. Castellano, L. Li, J.R. Lakowicz, Anal. Chem. 70 (1998) 632.
[13] J.D. Dattelbaum, O.O. Abugo, J.R. Lakowicz, Bioconjug. Chem. 11 (2000) 533.
[14] K.K. Lo, W.K. Hui, D.C. Ng, K.K. Cheung, Inorg. Chem. 41 (2002) 40.
[15] B. Rudolf, M. Palusiak, J. Zakrzewski, M. Salmain, G. Jaouen, Bioconjug. Chem. 16 (2005) 1218, and references therein.
[16] C.A. McPhalen, M.N.G. James, Acta Crystallogr., Sect. C 39 (1983) 1439.
[17] P. Hohenberg, W. Kohn, Phys. Rev. B 136 (1964) 864.
[18] W. Kohn, L.J. Sham, Phys. Rev. A 140 (1965) 1133.
[19] R.F.W. Bader, Atoms in Molecules. A Quantum Theory, Clarendon Press, Oxford, 1994.
[20] P. Popelier, Atoms in Molecules. An Introduction, Prentice-Hall, Englewood Cliffs, NJ, 2000.
[21] M.J. Frisch, G.W. Trucks, H.B. Schlegel, G.E. Scuseria, M.A. Robb, J.R. Cheeseman, V.G. Zakrzewski, J.A. Montgomery, R.E. Stratmann, J.C. Burant, S. Dapprich, J.M. Millam, A.D. Daniels, K.N. Kudin, M.C. Strain, O. Farkas, J. Tomasi, V. Barone, M. Cossi, R. Cammi, B. Mennucci, C. Pomelli, C. Adamo, S. Clifford, J. Ochterski, G.A. Petersson, P.Y. Ayala, Q. Cui, K. Morokuma, D.K. Malick, A.D. Rabuck, K. Raghavachari, J.B. Foresman, J. Cioslowski, J.V. Ortiz, B.B. Stefanov, G. Liu, A. Liashenko, P. Piskorz, I. Komaromi, R. Gomperts, L.R. Martin, D.J. Fox, T. Keith, M.A. Al-Laham, C.Y. Peng, A. Nanayakkara, G. Gonzalez, M. Challacombe, P.M.W. Gill, B. Johnson, W. Chen, M.W. Wong, J.L. Andres, C. Gonzalez, M. Head-Gordon, E.S. Replogle, J.A. Pople, GAUSSIAN-98, Revision A.6, Gaussian, Inc., Pittsburgh, PA, 1998.
[22] A.D. Becke, J. Chem. Phys. 98 (1993) 5648.
[23] C. Lee, W. Yang, R.G. Parr, Phys. Rev. B 37 (1988) 785.
[24] B. Miehlich, A. Savin, H. Stoll, H. Preuss, Chem. Phys. Lett. 157 (1989) 200.
[25] R. Krishnan, J.S. Binkley, R. Seeger, J.A. Pople, J. Chem. Phys. 72 (1980) 650.
[26] A.D. McLean, G.S. Chandler, J. Chem. Phys. 72 (1980) 5639.
[27] P.J. Hay, W.R. Wadt, J. Chem. Phys. 82 (1985) 270.
[28] W.R. Wadt, P.J. Hay, J. Chem. Phys. 82 (1985) 284.
[29] P.J. Hay, W.R. Wadt, J. Chem. Phys. 82 (1985) 299.
[30] C.M. Breneman, K.B. Wiberg, J. Comput. Chem. 11 (1990) 361.
[31] F. Biegler-König, AIM2000, University of Applied Sciences, Bielefeld, Germany.
[32] F.H. Allen, Acta Crystallogr., Sect. B 58 (2002) 380.
[33] B. Szewczyk, W.A. Sokalski, J. Chem. Phys. 117 (2002) 6952.
[34] F. Martin, H. Zipse, J. Comput. Chem. 26 (2005) 97.
[35] L.E. Sutton (Ed.), Table of Interatomic Distances and Configuration in Molecules and Ions, Chemical Society, London, 1965, Supplement 1956–1959, Special Publication No. 18.
[36] C. Bueno, M.R. Churchill, Inorg. Chem. 20 (1981) 2197.
[37] S.J. Grabowski, J. Phys. Org. Chem. 17 (2004) 18.
[38] S.J. Grabowski, J. Mol. Struct. 562 (2001) 137.